

Fe₃O₄@SiO₂-SO₃H nanocomposites: an efficient magnetically separable solid acid catalysts for esterification reaction

Jing Li, Hongxiao Zhao , Xufeng Hou, Wenjun Fa, Junhui Cai

Key Laboratory for Micro-Nano Energy Storage and Conversion Materials of Henan Province, College of Advanced Materials and Energy, Institute of Surface Micro and Nano Materials, Xuchang University, Henan 461000, People's Republic of China
✉ E-mail: hxzhao0915@126.com

Published in Micro & Nano Letters; Received on 8th August 2016; Accepted on 26th September 2016

Fe₃O₄@SiO₂-SO₃H nanocomposites were successfully synthesised as the efficient magnetically separable solid acid catalysts for an esterification reaction. The resultant catalysts were characterised by X-ray diffraction, scanning electron microscopy, transmission electron microscopy, Fourier-transform infrared spectroscopy, vibrating sample magnetometer (VSM), and nitrogen physical adsorption analyses [Brunauer–Emmett–Teller (BET) theory]. The catalytic activities of as-prepared Fe₃O₄@SiO₂-SO₃H nanocomposites were also investigated for the esterification of n-butyl acetate and isoamyl acetate. The acid esterification rate was confirmed by gas chromatography. The results showed that the Fe₃O₄@SiO₂-SO₃H nanocomposites can be as candidate catalysts for the concentrated H₂SO₄ for the esterification reaction of n-butyl alcohol or isoamyl alcohol. More importantly, the magnetic catalysts can be easily separated from the reaction system by a magnetic bar and reused at least three recycles without significant degradation of their activities.

1. Introduction: In the past decades, solid acid catalysts [1–3] have been attracted extensive interests as environmentally friendly replacements for their counterparts liquid mineral acids, such as H₂SO₄, which are highly toxic, corrosive and hazardous catalysts. A number of solid acid catalysts, such as zeolite molecular sieve (ZMS), heteropoly acids and oxide solid superacid, have been developed.

ZMS shows poor catalytic proprieties because of its low density and low accessibility of the acid sites [4]. Heteropoly acids exhibit high catalytic activity under mild conditions since they have a high intrinsic acidity [5]. However, the pollution exists during the process of producing and treating these catalysts. Oxide solid superacid has excellent catalytic performance due to its high acidity [6], but it is difficult to separate catalysts from reaction mixtures. Recently, SO₃H-functioned groups are introduced in solid acid catalysts and have outstanding catalytic properties for various organic synthesis reactions [7–10]. Therefore, developing a SO₃H-functioned-groups solid acid catalyst is significant for synthesis of important organic compounds [11].

On the other hands, the separation of the catalysts with a simple method is important for recycling causing significant economic and environmental benefits [12]. Compared with the filtration or centrifugation with the high loss of catalysts, the separation of magnetic materials, which take advantage of the magnetic properties, is simple and effective. To provide more candidates for solid acid catalysts, more magnetic core solid acid catalysts with high efficiency and stability need to be developed.

Fe₃O₄ nanoparticles are the most promising catalysts supports because of their superparamagnetism and high surface area, ease of surface modification, and low toxicity [13–15]. However, Fe₃O₄ nanoparticles tend to aggregate into large clusters due to their magnetic properties, which effects the performance of the total catalysts. The presence of silica atoms on the surface of the Fe₃O₄ nanoparticles can prevent their aggregation, avoid reacting with acid in the process of sulfonation. The Si-O become a bridge between magnetic core and functioned groups shell since SiO₂ have biocompatibility and protection effects [16–18]. Naeimi groups reported that Fe₃O₄ encapsulated-silica sulphonic acid nanoparticles were prepared using a simple and efficient method and revealed their potential application in biomedical field [19]. Xiong *et al.* [20] obtained Fe₃O₄@SiO₂-SO₃H by ionic

liquids facilitating the hydrolysis of cellulose. Kundu's group synthesised a new class of pyrazole in the presence of Fe₃O₄@SiO₂-SO₃H as solid acid catalyst [21]. These results all encouraged us to research Fe₃O₄@SiO₂-SO₃H nanocomposites for esterification reaction. Although esterification reaction is one of the most fundamental reactions in organic chemistry, it is important to catalytic esterification using an efficient magnetically separable solid acid as catalysts from both academic and industrial points of view [22]. To the best of our knowledge, there were no reports about Fe₃O₄@SiO₂-SO₃H catalysts for esterification reaction.

In this paper, we report that Fe₃O₄@SiO₂-SO₃H nanocomposites with SO₃H as the functionalised groups are an efficient magnetically separable catalysts for esterification reaction. The nanocomposites were characterised by X-ray diffraction (XRD), scanning electron microscopy (SEM), transmission electron microscopy (TEM), Fourier-transform infrared spectroscopy (FTIR), vibrating sample magnetometer (VSM), and nitrogen physical adsorption analyses [Brunauer–Emmett–Teller (BET) theory]. The catalytic activity of Fe₃O₄@SiO₂-SO₃H nanocomposites were tested for the esterification of n-butyl acetate and isoamyl acetate.

2. Experimental

2.1. Synthesis of Fe₃O₄@SiO₂-SO₃H nanocomposites

2.1.1. Preparation of nano-Fe₃O₄: Nano-Fe₃O₄ was prepared with a previously reported [23] and modified procedure. FeCl₃·6H₂O (2.16 g, 8 mmol) and trisodium citrate dihydrate (0.5 g, 1.7 mmol) were dissolved in ethylene glycol (EG, 20 ml) in a three-necked round-bottom flask with mechanical stirring. Meanwhile, NaAc·3H₂O (3.3 g) were dissolved in another ethylene glycol (EG, 20 ml) and added dropwise in the flask. The resultant solution was further mechanical stirred for 30 min and then transferred to a Teflon-lined stainless-steel autoclave. The autoclave was heated to 200 °C and maintained for 20 h, and then cooled to room temperature naturally. The obtained black precipitate was washed with ethanol and deionised water with the assistance of a magnet for several times and then dried under vacuum.

2.1.2. Synthesis of Fe₃O₄@SiO₂ nanocomposites: Fe₃O₄@SiO₂ nanocomposites were synthesised by a modified stöber sol-gel method [24, 25]. Typically, the freshly prepared Fe₃O₄ particle (0.5 g) were initially dispersed by ultrasonic vibration in 95%

ethanol (100 ml) in a three-necked round-bottom flask. Then aqueous ammonia (3 ml) was added and the mixed solution was mechanically stirred to obtain a homogeneous solution. Afterward, a solution of TEOS (2.5 ml) in 95% ethanol (50 ml) were shaken in a constant pressure funnel and was added in a drop-wise manner in the above mixture under continuous mechanical stirring. The reaction was allowed to proceed for 8 h under mechanical stirring. The resulting $\text{Fe}_3\text{O}_4@\text{SiO}_2$ powders were washed with ethanol by magnetic decantation for 3–4 times and dried at 60°C under vacuum overnight.

2.1.3. Preparation of $\text{Fe}_3\text{O}_4@\text{SiO}_2\text{-SO}_3\text{H}$ nanocomposites: $\text{Fe}_3\text{O}_4@\text{SiO}_2\text{-SO}_3\text{H}$ nanocomposites were obtained through reacting chlorosulfonic acid with $\text{Fe}_3\text{O}_4@\text{SiO}_2$. Firstly, $\text{Fe}_3\text{O}_4@\text{SiO}_2$ (0.5 g) powders were added to a three-necked round-bottom flask with methylene dichloride (15 ml) and N_2 atmosphere. At the same time, chlorosulfonic acid (0.5 ml) was moved to a beaker with methylene dichloride (10 ml) and the beaker was sealed with a preservative film and then mechanically stirred. The products were washed with methylene dichloride until no more white smoke emerged and then dried at 60°C under vacuum overnight.

2.2. Characterisation of $\text{Fe}_3\text{O}_4@\text{SiO}_2\text{-SO}_3\text{H}$ nanocomposites: XRD data were collected by a Bruker D8 Advance ($\text{Cu-K}\alpha$ radiation) with a step of 0.02° . The morphologies of the samples were studied by a Zeiss LS-15 SEM and a Philips-CM10 TEM. Fourier transform infrared spectroscopy (FTIR, Nicolet 6700) analysis was performed with KBr plates using a spectral resolution of 4 cm^{-1} in the wave number range of $500\text{--}4000\text{ cm}^{-1}$. The magnetic properties were measured by using VSM (Lake shore 7404) at room temperature. The specific surface areas and porous properties of the samples were measured at liquid nitrogen temperature using N_2 physical adsorption by the BET surface area analyser (Micromeritics Gemini 2380). The samples were dried at 80°C overnight and then degassed at 300°C for 2 h prior to the analysis of the surface areas.

2.3. Catalytic performance test: The catalytic application of $\text{Fe}_3\text{O}_4@\text{SiO}_2\text{-SO}_3\text{H}$ nanocomposites were investigated for the esterification reaction of *n*-butyl alcohol or isoamyl alcohol with glacial acetic acid. In a general procedure, *n*-butyl alcohol 2.35 ml (0.025 mol) or isoamyl alcohol 2.85 ml (0.025 mol), glacial acetic 1.5 ml (0.025 mol) and home-made catalysts 0.025 g or concentrated sulphuric acid 1.3 ml were weighed into a flask (25 ml), and then zeolite was added. The flask was heated and refluxed for 1 h and then cooled. Upon the completion of the reaction, the magnetic catalysts were separated from the solid crude products using an external magnet. After reaction, the

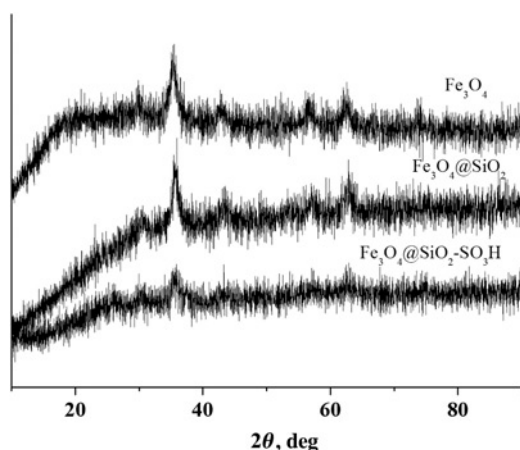


Fig. 1 XRD of the samples

catalyst was removed by an extra magnetic force and 1 ml of the residue mixture was taken out by an injection syringe and then filtered with a $0.5\text{ }\mu\text{m}$ syringe filter prior to analysis by gas chromatography (GC, GC122). The separated $\text{Fe}_3\text{O}_4\text{-SiO}_2\text{-SO}_3\text{H}$ was washed with water several times under ultrasonic for further catalysed reaction.

3. Results and discussion

3.1. Characterisation of the samples

3.1.1. XRD analysis: The powder XRD pattern of the products were shown in Fig. 1. The main peaks at $2\theta = 30.4^\circ$ (220), 35.5° (311), 43.4° (400), 57.2° (511), 62.7° (440) of the characteristics of Fe_3O_4 (JCPDS Card No. 3-862) can be observed in the three patterns indicating that the binding process did not induce a phase change. The XRD pattern of $\text{Fe}_3\text{O}_4@\text{SiO}_2\text{-SO}_3\text{H}$ nanocomposites shows obviously diffusion because of the existence of amorphous SO_3H .

3.1.2. Morphology analysis: The SEM and TEM micrographs of the products were presented in Figs. 2 and 3, respectively. From the SEM images of Fe_3O_4 nanoparticles, the sub-microspheres

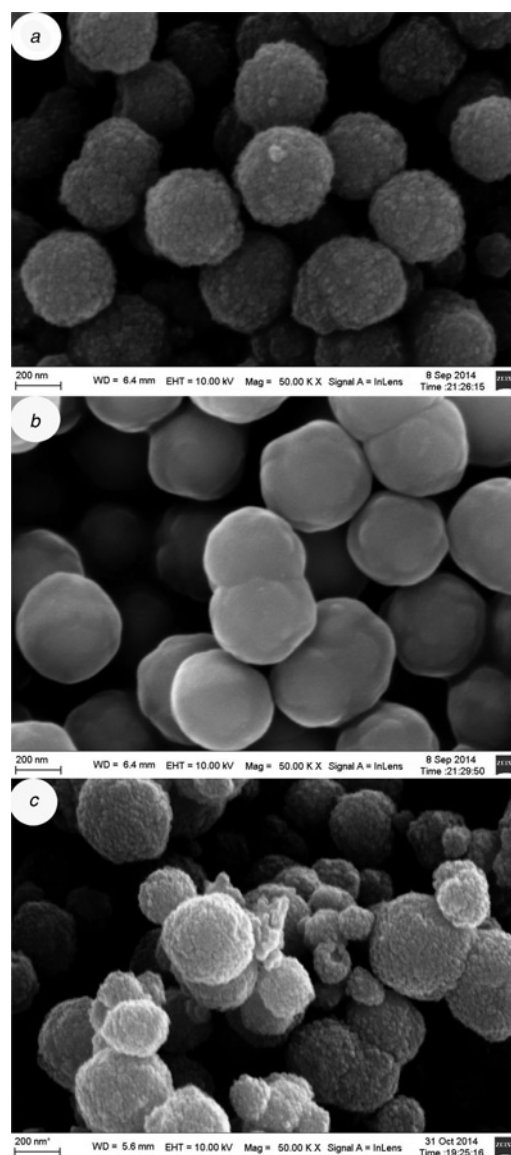


Fig. 2 SEM of
a Fe_3O_4 nanoparticles,
b $\text{Fe}_3\text{O}_4@\text{SiO}_2$ nanocomposites
c $\text{Fe}_3\text{O}_4@\text{SiO}_2\text{-SO}_3\text{H}$ nanocomposites

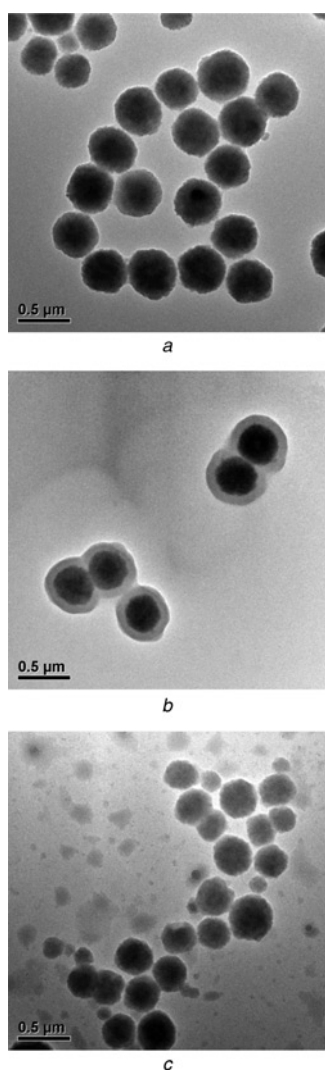


Fig. 3 TEM of the samples
a Fe_3O_4 nanoparticles,
b $\text{Fe}_3\text{O}_4@\text{SiO}_2$ nanocomposites
c $\text{Fe}_3\text{O}_4@\text{SiO}_2\text{-SO}_3\text{H}$ nanocomposites

with an average diameter of about 418 nm have been clearly observed. The spheres were composed of with the particles about

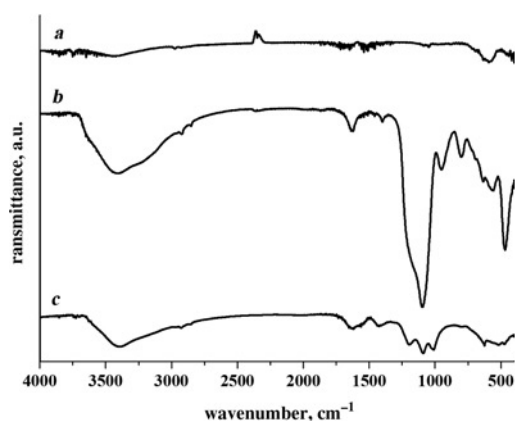


Fig. 4 FTIR of
a Fe_3O_4 nanoparticles
b $\text{Fe}_3\text{O}_4@\text{SiO}_2$ nanocomposites and
c $\text{Fe}_3\text{O}_4@\text{SiO}_2\text{-SO}_3\text{H}$ nanocomposites

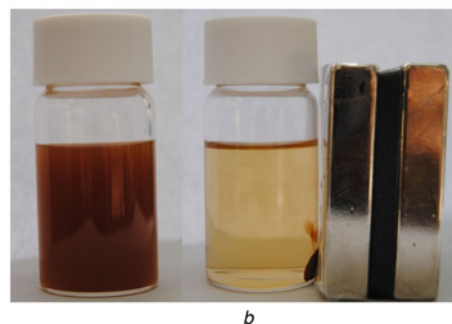
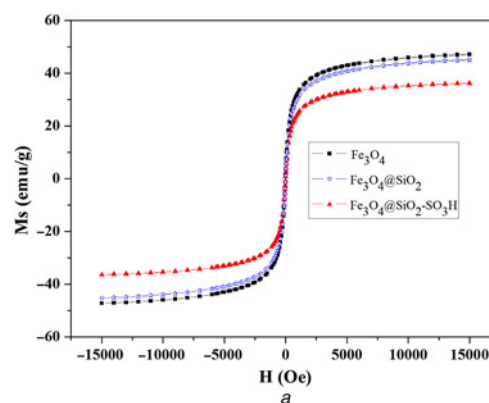


Fig. 5 The magnetic properties of the samples
a VSM measurement of the samples
b separation of $\text{Fe}_3\text{O}_4@\text{SiO}_2\text{-SO}_3\text{H}$ nanocomposites by external magnetic field

27 nm and the surfaces of such spheres appear to be slightly rough. A large variation has been found in the SEM image of $\text{Fe}_3\text{O}_4@\text{SiO}_2$ nanocomposites. The average diameter of $\text{Fe}_3\text{O}_4@\text{SiO}_2$ is ~ 472 nm and the surfaces of the microspheres are smoother than those of Fe_3O_4 , implied that the roughness of the surface of Fe_3O_4 microspheres got wiped out upon SiO_2 coating on them [26]. These results confirm the formation of the SiO_2 shell at the surface of Fe_3O_4 sub-microspheres. After SO_3H group were added, the products recovered slightly rough with the average diameter of 427 nm.

The TEM images indicate that the average diameter of Fe_3O_4 microspheres is ~ 418 nm. The TEM images of $\text{Fe}_3\text{O}_4@\text{SiO}_2$ confirms the core-shell structures with the core of 350 nm and the thickness of shell about 70 nm. In the case of $\text{Fe}_3\text{O}_4@\text{SiO}_2\text{-SO}_3\text{H}$ (Fig. 3c), the average diameter is 360 nm due to the amorphous of SO_3H coating over the $\text{Fe}_3\text{O}_4@\text{SiO}_2$ microspheres, the core-shell structures are not observed distinctly, which are in good accordance with XRD and SEM results.

3.1.3. FTIR spectra: The functionalisation of SiO_2 with Fe_3O_4 nanoparticles and $-\text{SO}_3\text{H}$ groups was further confirmed by FTIR (Fig. 4). A strong peak at 567 cm^{-1} along with a shoulder at 618 cm^{-1} are observed in the FTIR spectrum of Fe_3O_4 nanoparticles, which attributes to the stretching vibrational mode of the Fe–O functional group of Fe_3O_4 . While the strong asymmetric stretching vibration of Si–O–Si at 1080 cm^{-1} , symmetric vibration of Si–O–Si at 798 cm^{-1} and the symmetric stretching vibration of the Si–OH bond at 960 cm^{-1} are observed in the FTIR spectrum of $\text{Fe}_3\text{O}_4@\text{SiO}_2$ nanocomposites. By comparison, a sharp band around 1230 and 1050 cm^{-1} correspond to the O=S=O stretching vibration (Fig. 4c). The band around 630 cm^{-1} is seen for the S–OH stretching frequency. The broad band centred around 3400 cm^{-1} can be assigned to the stretching vibration of O–H of the free or absorbed water molecules. We speculate the formation of the

Table 1 BET surface area of the samples

Sample	Fe ₃ O ₄ nanoparticles	Fe ₃ O ₄ @SiO ₂ nanocomposites	Fe ₃ O ₄ @SiO ₂ -SO ₃ H nanocomposites
BET, m ² g ⁻¹	123.9	147.3	93.3

SiO₂ shell at the surface of Fe₃O₄ sub-microspheres, and SO₃H group were reacted to the surface of SiO₂.

3.1.4. Magnetic properties: It is of great importance that the composites should possess sufficient magnetic properties for its practical applications. Magnetic hysteresis measurements for the samples were done in an applied magnetic field with the fields at room temperature, with the sweeping from -15,000 to +15,000 Oe. As shown in Fig. 5a, the M (H) hysteresis loop for the samples was completely reversible, showing that the three products exhibit superparamagnetic characteristics. The hysteresis loops of them reached saturation up to the maximum applied magnetic field. The saturation magnetisation values of Fe₃O₄@SiO₂ nanocomposites was about 45.22 emu g⁻¹ and it was reduced to 36.36 emu g⁻¹ after supporting with SO₃H. Both of these values were lower than the initial value of Fe₃O₄ nanoparticles (47.28 emu g⁻¹). The decrease of the saturation magnetisation after the coating of Fe₃O₄ nanoparticles confirms the presence of a diamagnetic outer shell (SiO₂ or SiO₂-SO₃H). However, the magnetic saturation value of Fe₃O₄@SiO₂ nanocomposites is higher than that in literature [27] and it is sufficient for magnetic separation with a conventional magnet (as shown in the inset image of Fig. 5b).

3.1.5. BET analysis: The surface area (BET) was determined by the nitrogen physical adsorption and were carried out at liquid nitrogen boiling point. The surface area of Fe₃O₄ nanoparticles, Fe₃O₄@SiO₂ nanocomposites and Fe₃O₄@SiO₂-SO₃H nanocomposites is 123.9, 147.3 and 93.3 m² g⁻¹, respectively (Table 1). It is worth noting that the reducing surface area is a consequence of successful immobilising SO₃H onto the surface of silica coated Fe₃O₄ nanoparticles, which is in agreement with FTIR result.

3.2. Catalytic study: The catalytic properties of Fe₃O₄@SiO₂-SO₃H nanocomposites and concentrated H₂SO₄ for different esterification reaction were studied by GC and the esterification rate was obtained (Fig. 6). From Fig. 6, it can be seen that the catalytic performance of Fe₃O₄@SiO₂-SO₃H catalysts and that of the concentrated sulphuric acid for esterification reaction is equal. The recovering and reusability test of Fe₃O₄@SiO₂-SO₃H nanocomposites catalysts were also carried out and the results were shown in Fig. 7. The

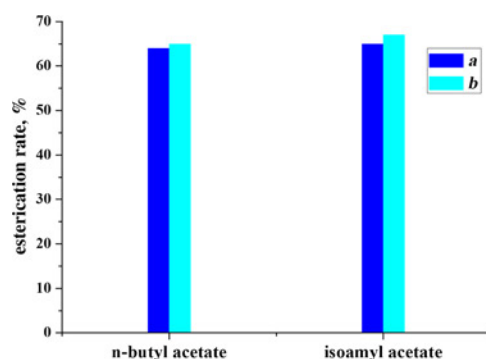


Fig. 6 Esterification rate of different catalysts
a Fe₃O₄@SiO₂-SO₃H nanocomposites
b concentrated H₂SO₄

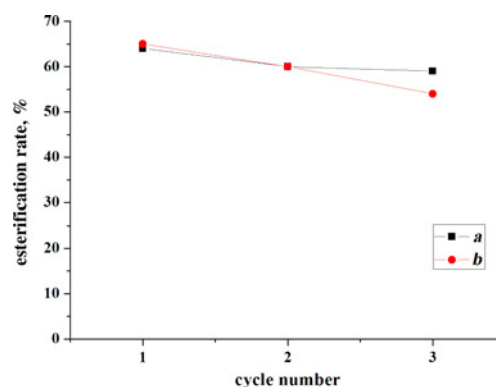


Fig. 7 Reusability test of Fe₃O₄@SiO₂-SO₃H nanocomposites for different esterification reaction
a n-butyl acetate;
b isoamyl acetate

results showed that there is indeed substantial retention of initial catalytic activity of Fe₃O₄@SiO₂-SO₃H nanocomposites even after 3 times.

4. Conclusion: In summary, Fe₃O₄@SiO₂-SO₃H nanocomposites have been successfully achieved and can be used for the esterification reaction. The catalysts are inexpensive and easy to prepare. The Fe₃O₄@SiO₂-SO₃H nanocomposites have the high catalytic efficiency for the esterification reaction of n-butyl alcohol or isoamyl alcohol, which can be as candidate catalysts for the concentrated H₂SO₄. In addition, they can be easily separated from the reaction mixture and reused three recycle without any significant loss on their activity. Fe₃O₄@SiO₂-SO₃H nanocomposites is safer in terms of toxicity and more environmental acceptability than other conventional catalysts. These catalysts can be used as ideal materials for esterification reaction in future.

5. Acknowledgments: This work was financially supported by the National Natural Science Foundation of China (grant no. 21273192), Innovation Scientists and Technicians Troop Construction Projects of Henan Province (grant no. 144200510014), Program for Innovative Research Team (in Science and Technology) in University of Henan Province (grant no. 2012IRTSTHN021), Henan Province Science and Technology Key Project (grant no. 122102210479).

6 References

- [1] Harmer M.A., Sun Q., Michalczyk M.J., *ET AL.*: 'Unique silane modified perfluorosulfonic acids as versatile reagents for new solid acid catalysts', *Chem. Commun.*, 1997, pp. 1803–1804
- [2] Takagaki A., Tagusagawa C., Hayashi S., *ET AL.*: 'Nanosheets as highly active solid acid catalysts for green chemical syntheses', *Energy Environ. Sci.*, 2010, **3**, pp. 82–93
- [3] Zheng A., Huang S.J., Liu S.B., *ET AL.*: 'Acid properties of solid acid catalysts characterized by solid-state ³¹P NMR of adsorbed phosphorous probe molecules', *Phys. Chem. Chem. Phys.*, 2011, **13**, pp. 14889–14901
- [4] Zillillah Tan G., Li Z.: 'Highly active, stable, and recyclable magnetic nano-size solid acid catalysts: efficient esterification of free fatty acid in grease to produce biodiesel', *Green Chem.*, 2012, **14**, pp. 3077–3086
- [5] Vu T.H.T., Au H.T., Nguyen T.M.T., *ET AL.*: 'Esterification of 2-keto-L-gulonic acid catalyzed by a solid heteropoly acid', *Catal. Sci. Technol.*, 2013, **3**, pp. 699–705
- [6] Hino M., Arata K.: 'Synthesis of solid superacid of tungsten oxide supported on zirconia and its catalytic action for reactions of butane and pentane', *J. Chem. Soc., Chem. Commun.*, 1988, pp. 1259–1260
- [7] Amoozadeh A., Golian S., Rahmani S.: 'TiO₂-coated magnetite nanoparticle-supported sulfonic acid as a new, efficient, magnetically

- separable and reusable heterogeneous solid acid catalyst for multi-component reactions', *RSC Adv.*, 2015, **5**, pp. 45974–45982
- [8] Ryoo H.I., Hong L.Y., Jung S.H., *ET AL.*: 'Direct syntheses of sulfonated mesoporous SiO₂-TiO₂-SO₃H materials as solid acid catalysts', *J. Mater. Chem.*, 2010, **20**, pp. 6419–6421
- [9] Li P., Cao C.Y., Liu H., *ET AL.*: 'Synthesis of a core-shell-shell structured acid-base bifunctional mesoporous silica nanoreactor (MS-SO₃H@MS@MS-NH₂) and its application in tandem catalysis', *J. Mater. Chem. A*, 2013, **1**, pp. 12804–12810
- [10] Russo P.A., Antunes M.M., Neves P., *ET AL.*: 'Solid acids with SO₃H groups and tunable surface properties: versatile catalysts for biomass conversion', *J. Mater. Chem. A*, 2014, **2**, pp. 11813–11824
- [11] Debnath K., Singha K., Pramanik A.: 'Magnetically separable Fe₃O₄-SO₃H nanoparticles as an efficient solid acid support for the facile synthesis of two types of spiroindole fused dihydropyridine derivatives under solvent free conditions', *RSC Adv.*, 2015, **5**, pp. 31866–31877
- [12] Rostamnia S., Lamei K., Mohammadquli M., *ET AL.*: 'Nanomagnetically modified sulfuric acid (γ-Fe₂O₃@SiO₂-OSO₃H): an efficient, fast, and reusable green catalyst for the Ugi-like Groebke-Blackburn-Bienaymé three-component reaction under solvent-free conditions', *Tetrahedron Lett.*, 2012, **53**, pp. 5257–5260
- [13] Bamoniri A., Moshtael-Arani N.: 'Nano-Fe₃O₄ encapsulated-silica supported boron trifluoride as a novel heterogeneous solid acid for solvent-free synthesis of arylazo-1-naphthol derivatives', *RSC Adv.*, 2015, **5**, pp. 16911–16920
- [14] Zeng T., Chen W.W., Cirtiu C.M., *ET AL.*: 'Fe₃O₄ nanoparticles: a robust and magnetically recoverable catalyst for three-component coupling of aldehyde, alkyne and amine', *Green Chem.*, 2010, **12**, pp. 570–573
- [15] Shen P., Zhang H.T., Liu H., *ET AL.*: 'Core-shell Fe₃O₄@SiO₂@HNbMoO₆ nanocomposites: new magnetically recyclable solid acid for heterogeneous catalysis', *J. Mater. Chem. A*, 2015, **3**, pp. 3456–3464
- [16] Wei Y., Yang R., Zhang Y.X., *ET AL.*: 'High adsorptive γ-AlOOH (boehmite)@SiO₂/Fe₃O₄ porous magnetic microspheres for detection of toxic metal ions in drinking water', *Chem. Commun.*, 2011, **47**, pp. 11062–11064
- [17] Zhang Y., Yu M., Zhang C., *ET AL.*: 'Highly specific enrichment of N-glycoproteome through a nonreductive amination reaction using Fe₃O₄@SiO₂-aniline nanoparticles', *Chem. Commun.*, 2015, **51**, pp. 5982–5985
- [18] Naeimi H., Aghaseyedikarimi D.: 'Highly specific enrichment of N-glycoproteome through a nonreductive amination reaction using Fe₃O₄@SiO₂-aniline nanoparticles', *New J. Chem.*, 2015, **39**, pp. 9415–9421
- [19] Naeimi H., Nazifi Z.S., Amininezhad S.M.: 'Preparation of Fe₃O₄ encapsulated-silica sulfonic acid nanoparticles and study of their in vitro antimicrobial activity', *J. Photochem. Photobiol. B Biol.*, 2015, **149**, pp. 180–188
- [20] Xiong Y., Zhang Z., Wang X., *ET AL.*: 'Hydrolysis of cellulose in ionic liquids catalyzed by a magnetically-recoverable solid acid catalyst', *Chem. Eng. J.*, 2014, **235**, pp. 349–355
- [21] Kundu A., Mukherjee S., Pramanik A.: 'Synthesis of a new class of pyrazole embedded spirocyclic scaffolds using magnetically separable Fe₃O₄@SiO₂-SO₃H nanoparticles as recyclable solid acid support', *RSC Adv.*, 2015, **5**, pp. 107847–107856
- [22] Thombal R.S., Jadhav A.R., Jadhav V.H.: 'Biomass derived β-cyclodextrin-SO₃H as a solid acid catalyst for esterification of carboxylic acids with alcohols', *RSC Adv.*, 2015, **5**, pp. 12981–12986
- [23] Liu J., Sun Z., Deng Y., *ET AL.*: 'Highlywater-dispersible biocompatible magnetite particles with low cytotoxicity stabilized by citrate groups', *Angew. Chem. Int. Ed.*, 2009, **48**, pp. 5875–5879
- [24] Liu J., Xu J., Che R., *ET AL.*: 'Hierarchical Fe₃O₄@TiO₂ yolk-shell microspheres with enhanced microwave-absorption properties', *Chem. Eur. J.*, 2013, **19**, pp. 6746–6752
- [25] Liu J., Xu J., Che R., *ET AL.*: 'Hierarchical magnetic yolk-shell microspheres with mixed barium silicate and barium titanium oxide shells for microwave absorption enhancement', *J. Mater. Chem.*, 2012, **22**, pp. 9277–9284
- [26] Majumder S., Dey S., Bagani K., *ET AL.*: 'A comparative study on the structural, optical and magnetic properties of Fe₃O₄ and Fe₃O₄@SiO₂ core-shell microspheres along with an assessment of their potentiality as electrochemical double layer capacitors', *Dalton Trans.*, 2015, **44**, pp. 7190–7202
- [27] Eshghi H., Khojastehnezhad A., Moeinpour F., *ET AL.*: 'Synthesis, characterization and first application of keggins-type heteropoly acids supported on silica coated NiFe₂O₄ as novel magnetically catalysts for the synthesis of tetrahydropyridines', *RSC Adv.*, 2014, **4**, pp. 39782–39789